COBEM 2023 27TH INTERNATIONAL CONGRESS OF MECHANICAL ENGENEERING

ABCM Brazilian Society of Mechanical Sciences and Engineering
27th ABCM International Congress of Mechanical Engineering
December 04-08, 2023, Florianópolis-SC, Brazil

COB-2023-0211
NUMERICAL THERMOMECHANICAL ANALYSIS OF A COMPOSITE SANDWICH BEAM

Lucas Antonio de Oliveira
lucasoliveira2@unifei.edu.br
Rafael Augusto Gomes
Mechanical Engineering Institute, Federal University of Itajuba (UNIFEI), Av. BPS, 1303, Itajuba, 37500-903, Minas Gerais, Brazil
d2022103026@unifei.edu.br

Matheus Brendom Francisco
Institute of Industrial Engineering and Management, Federal University of Itajubá (UNIFEI), Av. BPS, 1303, Itajuba, 37500-903, Minas Gerais, Brasil
matheus brendon@unifei.edu.br

Guilherme Ferreira Gomes
guilhermefergom@unifei.edu.br
Sebastião Simões da Cunha Junior
Mechanical Engineering Institute, Federal University of Itajuba (UNIFEI), Av. BPS, 1303, Itajuba, 37500-903, Minas Gerais, Brazil
sebas@unifei.edu.br

Abstract. *If composite materials are to be used safely and perform at a high level, existing internal damage must be detected. Therefore, viscoelastic characteristics can be exploited during cyclic loading of the material. Both internal heat generation (induced by hysteresis), resulting from the application of loading cycles, as well as thermal conductivity and specific mass, are intrinsic characteristics of the material but may present variations in regions with defects. Therefore, the choice of the parameters that make up the excitation signal (amplitude and natural frequency) and the characterization of the individual properties of the materials that make up the structure are necessary for the study. From the excitation signal obtained from the modal analysis, the maximum stresses per cycle obtained in the nodes generated by the finite element method, the thermal properties, and the modulus of material loss resulting from heat dissipation by hysteresis obtained experimentally in the laboratory, it is possible to determine the temperature increment per node of the structure. As a result of these procedures, an analysis of the temperature profile on the material surface is performed, which will allow for the detection of damage near the structure's surface.*

Keywords: *Vibrothermography, Viscoelastic, Composite, Non-Destructive, MEF*

1. INTRODUCTION

The knowledge about the response of sandwich structures to applications that require, among other characteristics, a good strength-to-weight ratio or good energy absorption capacity ((Sun *et al.*, 2019), (Zhang *et al.*, 2018), (Xia *et al.*, 2023)), allows technological advances in the aerospace, automotive, and marine industries, among others. In addition to knowledge of the stresses to which the structure will be exposed, performing inspections that seek to quantify and locate damage present in structures is essential for efficient and safe use. Thus, to determine the real structural conditions, some methodologies or analysis tools can be used, such as "active" or "passive" infrared thermography(IRT) (Harizi *et al.* (2014), Ramzan *et al.* (2021)), acoustic emission (AE), and the realization of a post-processing.

In the analysis of possible damage to the structure, different methods or techniques are used, such as experimental analysis, numerical simulation, or a combination of these. In your work, Dikshit *et al.* (2021) analyzed two structures manufactured using fused filament fabrication (FFF) and inkjet printing techniques. Sandwich-1 and sadwich-2 were structures with trapezoidally vertically pillared and sinusoidally vertically pillared designs, respectively. For the analysis of the specimen manufactured, structural health monitoring was performed using the non-destructive (ND) acoustic emission technique, in addition to micro-computed tomography to detect failure points and damage propagation.

Tříska *et al.* (2021) used active infrared thermography to analyze the heating generated in the sandwich structure after applying internal excitation using a thin-film resistive heating element, in addition to performing a numerical simulation. It was shown that the detection is possible with the use of the thin-film resistive heating element without the need for external excitation sources; however, the detection of the damages depends on the disposition and type of the damages in

the structure.

Ramakrishnan *et al.* (2021) has already studied the use or non-use of nano-reinforced composite facesheets in numerical modeling to investigate the response to low-velocity impact damage. The response of the sandwich panels with nanoparticles (Kevlar-Nanostrength-Rohacell, KNR) or without nanoparticles (Kevlar-Rohacell, KR) had good results and can be used in other conditions.

Therefore, many types of techniques can be used to detect this damage in composite materials, vibrothermography being one of them. This technique, which uses vibration to excite the structure and thermography to map the surface of the materials, is used to detect damage in composite materials, as presented in de Oliveira *et al.* (2023). Thus, this paper presents the analysis of the temperature profile generated on the surface of the material after using the vibrothermography technique.

2. MODELING AND METHODS

2.1 MODELING

The design of the sandwich beam was performed using computer-aided engineering (CAE) software, which allowed the modeling and numerical analysis of the beam. This is composed of the materials PREPREG and ROHACELL HERO 71®, whose configuration presents the PREPREG material at the ends and ROHACELL HERO 71®, located in the middle of the structure (Fig. 1).

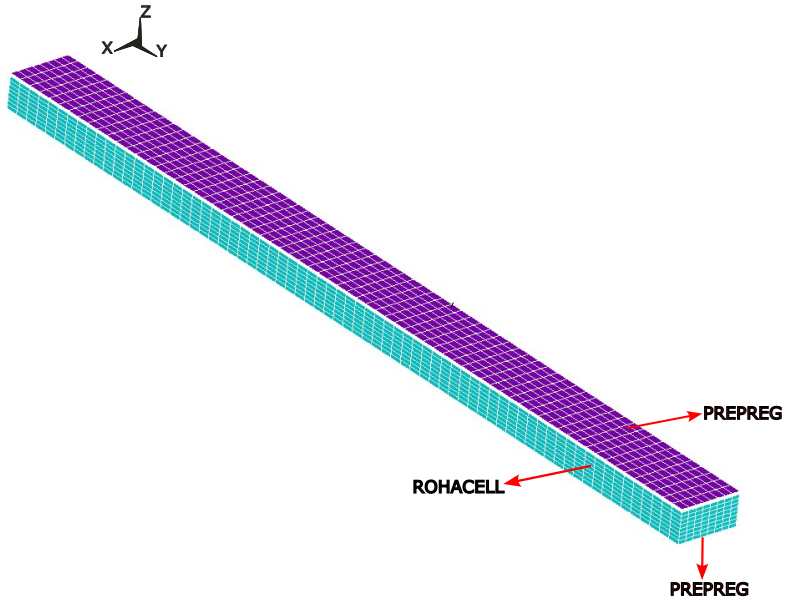

Figure 1. Sandwich beam

The properties of the materials and the dimensions of the beam are presented in the Tabs. 1 and 2, respectively.

Table 1. Properties of the materials.

Material	Properties		Value	Unit
ROHACELL HERO 71®	Tensile Modulus	E_T	123	MPa
	Compressive Modulus	E_c	48	MPa
	Shear modulus	G	28	MPa
	Density	ρ	75.0	kg/m^3
	Poisson Coefficient	ν	0.25	-
PREPREG	Tensile Modulus	E_T	1089	MPa
	Compressive Modulus	E_c	674	MPa
	Shear modulus	G	67.8	MPa
	Density	ρ_1	1510	kg/m^3
	laminate thickness	e_1	0.0012	m

Table 2. Dimensions of the sandwich beam.

Dimension	Value	Unit
Lenght	0.360	m
Widht	0.025	m
Tickness	0.0151	m

2.2 METHODS

2.2.1 DEFINITION OF THE BOUNDARY CONDITION

To start the analysis, some boundary conditions must be applied, i.e., the region of fixing and the point of application of the cyclic loading must be known. For this purpose, Fig. 2 shows the position of the fixing at one end of the sandwich beam and the location of the damage in an ellipse shape inserted under the carbon layer. The damage was defined by applying different mechanical and thermal properties to the materials that compose the sandwich beam, and its location was chosen away from the crimping region and away from the region of application of cyclic loads to avoid the regions of higher intensity of stresses generated in the beam during loading. This choice is important both to compare the location of the temperature profile generated on the surface of the material with the location of the damage in the beam and to move the damage away from the points of higher temperature increment that can make its identification difficult.

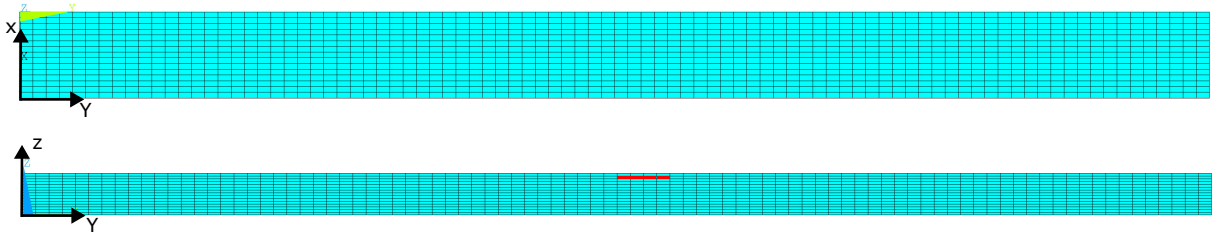

Figure 2. Locating the damage and fixing the beam.

2.2.2 DEFINITION OF THE NATURAL FREQUENCIES

From the structure defined above, the first ten vibration modes were obtained from modal analysis, and their values are presented in Tab. 3. For better understanding and visualization of the vibration modes, some of the bending modes are presented from the Frequency Response Function (FRF) (Fig. 3) measured perpendicular to the xy orientation plane and from Fig.4, where we can observe the manifestation of the modes at frequencies 124.69, 456.27, 925.62, 1397.75, and 1928.04 Hz, respectively. These frequency values can be used for the calculation of the temperature variation at the beam nodes (the acquisition of the other modes must be performed in the x or y directions).

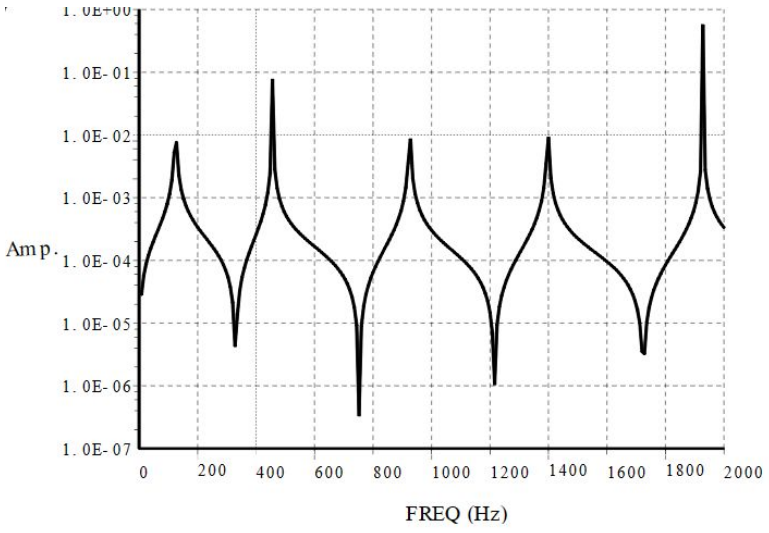

Figure 3. Modal test.

Table 3. Vibration modes obtained from the software.

Modes	Frequency (Hz)	Modes	Frequency (Hz)
1°	124.69	6°	1071.31
2°	187.07	7°	1215.06
3°	372.26	8°	1397.75
4°	456.27	9°	1928.04
5°	925.62	10°	2275.17

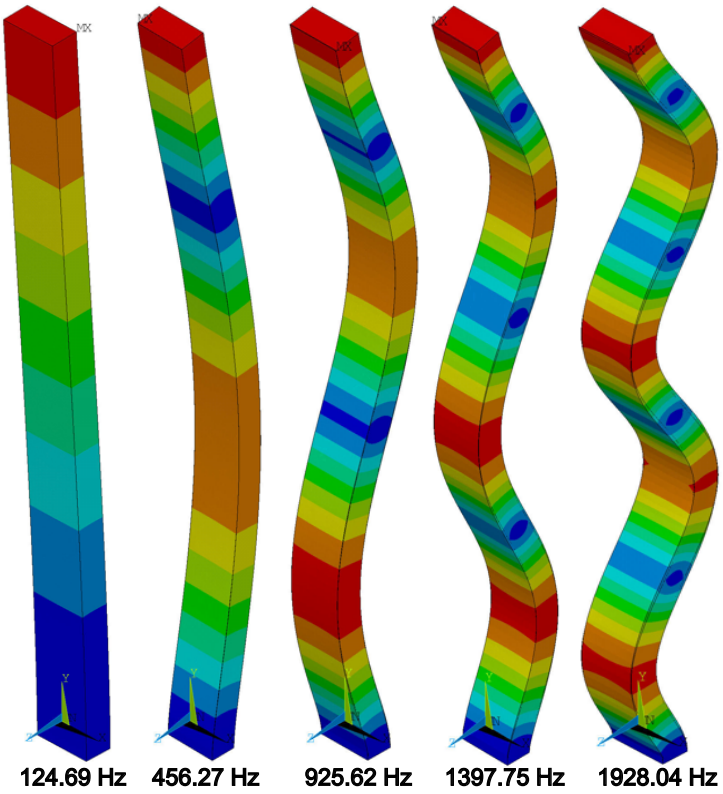

Figure 4. Modal shapes - xy bending plane.

2.2.3 FORMULATION OF THE INTERNAL HEAT GENERATION IN THE SAMPLE

In this step, some parameters, such as the loss modulus and the natural frequencies, must be obtained for the implementation of the equations. Thus, in addition to defining the force (Eq. 1) that will excite the specimen, it is necessary to define the loss modulus (Eq. 2), which, unlike the storage modulus (Eq. 3), which represents the material's ability to store energy elastically, represents the material's ability to dissipate heat through stress, is a variable present in the calculation of temperature variation, and its use can be found in the studies of Gupta *et al.* (2020), Puentes *et al.* (2019) and Szmidt *et al.* (2017) .

$$F(t) = A \cdot sin(\omega \cdot t) \tag{1}$$

Figure 5 besides presenting the profile of the loading applied to the free end of the beam, is composed of the natural frequency of vibration obtained by modal analysis and also presents the displacement generated in the structure in a given time.

$$E''(\omega, T) = \omega \cdot \int_0^\infty E(t, T) \cdot cos(\omega \cdot t)\, dt \tag{2}$$

$$E'(\omega, T) = \omega \cdot \int_0^\infty E(t, T) \cdot sin(\omega \cdot t)\, dt \tag{3}$$

where A and ω are the amplitude and frequency applied to the specimen, respectively.

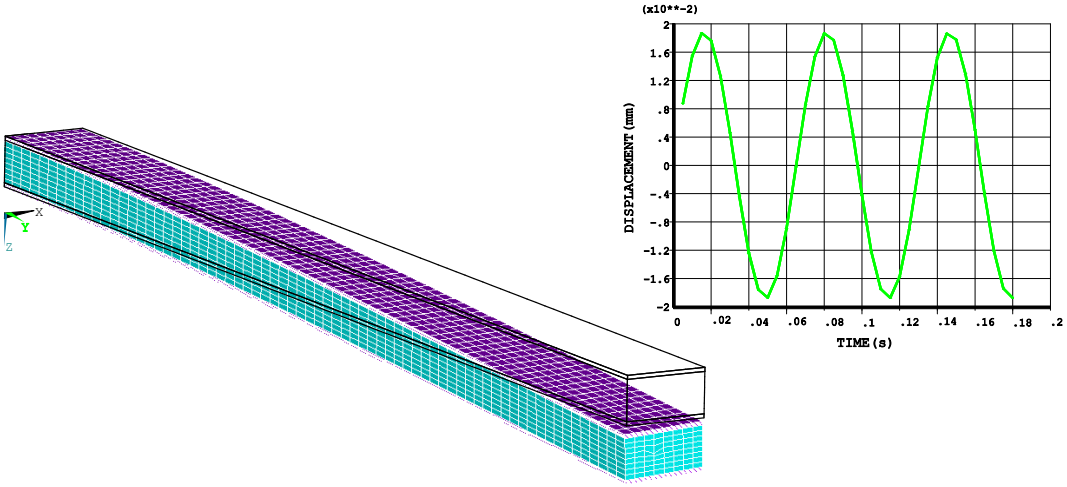

Figure 5. Displacement and applied load.

As shown in Eq. 4, the complex module is the sum of the storage and loss modules, and the difference in phase among the responses of these parameters is defined as phase lag, while your tangent indicates the relative degree of energy dissipation or damping of the material, Eq. 5 (Franck and Germany (1993)).

$$E^{+} = E'(\omega, T) + i \cdot E''(\omega, T) \tag{4}$$

$$tg(\delta) = \frac{E''(\omega,T)}{E'(\omega,T)} \tag{5}$$

Therefore, became possible calculate the dissipated energy Eq. 6 and the temperature variation of the specimen Eq. 7.

$$Q_d(t) = \frac{\omega}{2 \cdot \pi} \cdot \int_0^{\frac{2 \cdot \pi}{\omega}} \sigma(t) \cdot \frac{d\varepsilon(t)}{dt}\, dt \tag{6}$$

$$\Delta \dot{T} = \frac{\omega \cdot E''(\omega \cdot t) \cdot \sigma_{max}^2}{\pi \cdot \rho(T) \cdot c(T)} \tag{7}$$

According to Eq. 7, the temperature variation is related to the highest stress encountered per cycle, the loss modulus, and the frequency applied to the specimen, in addition to the mechanical properties of the material. Thus, even if the mechanical properties, frequency, and loss modulus are the same for the calculation of the temperature variation, the different stresses found in each element of the specimen will be responsible for the different temperatures generated. As a result, it is expected that when the specimen is free of internal damage, the temperature distribution should be uniform with no significant temperature variation across the specimen, which should be different when there is damage to the structure.

3. RESULTS AND DISCUSSIONS

In this section, the two results of the analysis are presented separately in order to better show the results.

3.1 STRESS INTENSITY PROFILE

After fixing one of the ends of the specimen, the application of cyclic loads in the z direction induced stresses throughout the structure, which allowed measuring the highest stress intensity generated at each node of the mesh per loading cycle.

After applying the cyclic loading and choosing the point of major displacement shown by the beam, it became possible to obtain the stress intensity profile. According to what is presented in Fig. 6, near the fixed end the highest stresses are generated, and near the free end the lowest stresses are generated, except in the load application region. Due to the different properties found in the damage region located within the sandwich beam, the different stress intensities generated will result in a discontinuity in the temperature field.

3.2 TEMPERATURE PROFILE

From the utilization of the equations Using the equations described in Section 2.2.3, and the stress intensity obtained during mechanical excitation, the respective temperature increment is found for each node of the discretized structure.

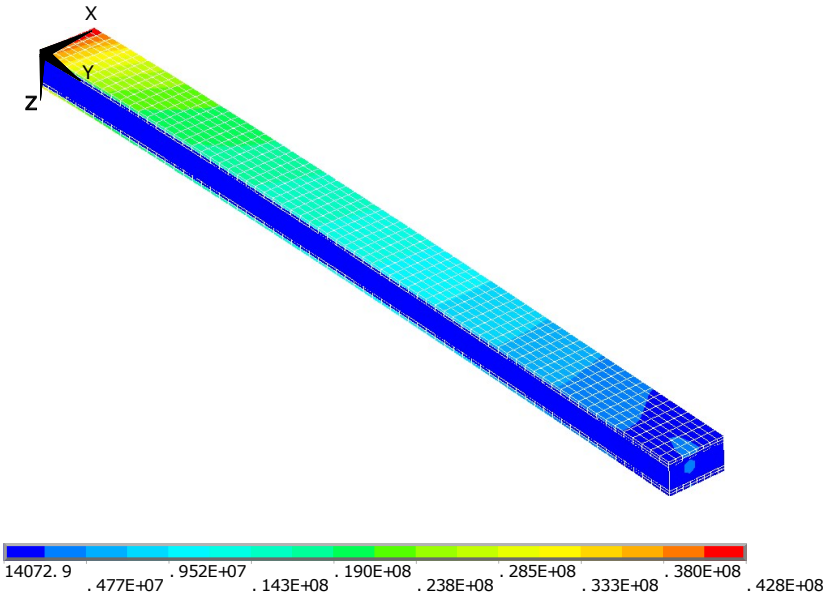

Figure 6. Stress Intensity (Pa).

Thus, the simulation of the thermal behavior carried out after obtaining the information from the mechanical excitation simulation provides information on the possible areas of damage to the structure.

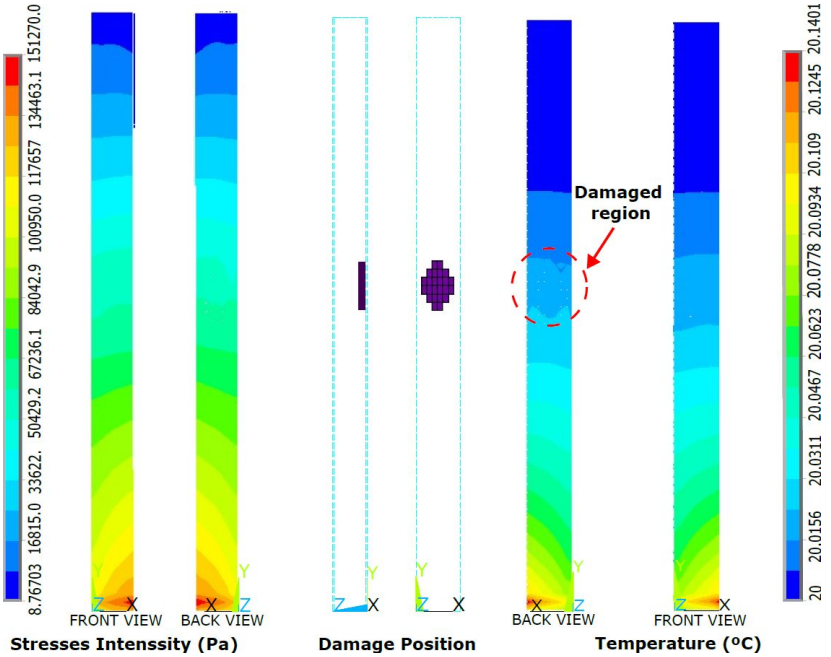

Figure 7. Temperature profile

As presented by Fig. 7, the temperature profile varies according to the local stress in the structure. Thus, in the damaged region, a different temperature profile is generated on the surface of the material.

4. CONCLUSION

The use of the vibrothermography technique to excite the structure with a sinusoidal signal showed good results. After applying the excitation and generating the stress profile in the structure, the thermal simulation response made it possible to detect changes in the temperature gradient observed on the surface of the material. The different properties attributed to the damaged elements showed correspondence with the stress generated, since the heat dissipation presented by the structure during each excitation cycle, with the contribution of the viscoelastic response, made it possible to identify the presence of the damage attributed to the structure. Other changes can be made to improve detection, such as how the combination of natural frequencies alters the type of signal excited. With post-processing in mind, optimization methods can be used to improve characterization and detect further damage.

5. ACKNOWLEDGEMENTS

The authors would like to acknowledge the financial support from the Brazilian agencies: CAPES (Coordenação de Aperfeiçoamento de Pessoal de Nível Superior), CNPq(Conselho Nacional de Desenvolvimento Científico e Tecnológico), FAPEMIG (Fundação de Amparo à Pesquisa do Estado de Minas Gerais, Grant number APQ-00385-18). The authors would also like to acknowledge of the Tutorial Educatin Program (PET - Programa de Educação Tutorial).

6. REFERENCES

de Oliveira, L.A., Gomes, G.F., Pereira, J.L.J., Francisco, M.B., Demarbaix, A. and Cunha Jr, S.S., 2023. "New trends of damage detection and identification based on vibrothermography in composite materials". *Journal of Nondestructive Evaluation*, Vol. 42, No. 3, p. 57.

Dikshit, V., Nagalingam, A.P., Goh, G.D., Agarwala, S., Yeong, W.Y. and Wei, J., 2021. "Quasi-static indentation analysis on three-dimensional printed continuous-fiber sandwich composites". *Journal of Sandwich Structures & Materials*, Vol. 23, No. 2, pp. 385–404. doi:10.1177/1099636219836058.

Franck, A. and Germany, T., 1993. "Viscoelasticity and dynamic mechanical testing". *TA Instruments, New Castle, DE, USA AN004*.

Gupta, A., Panda, S. and Reddy, R.S., 2020. "Improved damping in sandwich beams through the inclusion of dispersed graphite particles within the viscoelastic core". *Composite Structures*, Vol. 247, p. 112424.

Harizi, W., Chaki, S., Bourse, G. and Ourak, M., 2014. "Mechanical damage assessment of glass fiber-reinforced polymer composites using passive infrared thermography". *Composites Part B: Engineering*, Vol. 59, pp. 74–79.

Puentes, J., Quintana, J.L.C., Chaloupka, A., Rudolph, N. and Osswald, T.A., 2019. "Moduli development of epoxy adhesives during cure". *Polymer Testing*, Vol. 77, p. 105863.

Ramakrishnan, K.R., Guérard, S., Zhang, Z., Shankar, K. and Viot, P., 2021. "Numerical modelling of foam-core sandwich panels with nano-reinforced composite facesheets". *Journal of Sandwich Structures & Materials*, Vol. 23, No. 4, pp. 1166–1191. doi:10.1177/1099636219856537.

Ramzan, B., Malik, M.S., Martarelli, M., Ali, H.T., Yusuf, M. and Ahmad, S., 2021. "Pixel frequency based railroad surface flaw detection using active infrared thermography for structural health monitoring". *Case Studies in Thermal Engineering*, Vol. 27, p. 101234.

Sun, M., Wowk, D., Mechefske, C. and Kim, I.Y., 2019. "An analytical study of the plasticity of sandwich honeycomb panels subjected to low-velocity impact". *Composites Part B: Engineering*, Vol. 168, pp. 121–128.

Szmidt, T., Pisarski, D., Bajer, C. and Dyniewicz, B., 2017. "Double-beam cantilever structure with embedded intelligent damping block: Dynamics and control". *Journal of Sound and Vibration*, Vol. 401, pp. 127–138.

Tříska, V., Chlebeček, T., Hnidka, J. and Maňas, K., 2021. "Testing of the heating element integrated into the honeycomb sandwich structure for active thermography inspection". *Journal of Sandwich Structures & Materials*, Vol. 23, No. 7, pp. 3368–3389. doi:10.1177/1099636220927888.

Xia, H., Sun, Q. and Wang, S., 2023. "Influence of strain rate effect on energy absorption characteristics of bio-inspired honeycomb column thin-walled structure under impact loading". *Case Studies in Construction Materials*, Vol. 18, p. e01761. ISSN 2214-5095. doi:https://doi.org/10.1016/j.cscm.2022.e01761.

Zhang, J., Ye, Y., Qin, Q. and Wang, T., 2018. "Low-velocity impact of sandwich beams with fibre-metal laminate face-sheets". *Composites Science and Technology*, Vol. 168, pp. 152–159. ISSN 0266-3538. doi: https://doi.org/10.1016/j.compscitech.2018.09.018.

7. RESPONSIBILITY NOTICE

The author(s) is (are) the only responsible for the printed material included in this paper.